Impact of whitecap coverage derived from a wave model on the assimilation of radiances from microwave imagers

Louis-François Meunier[a], Stephen English[b], and Peter Janssen[b]

[a]Météo-France and CNRS,CNRM-GAME/GMAP, Toulouse, France
[b]European Centre for Medium-Range Weather Forecasts, Reading, United Kingdom

June 3, 2014

Abstract The assimilation of radiances from microwave imagers, relies on an accurate representation of the surface properties in a radiative transfer model. The ECMWF IFS 4D-Var assimilation system uses the RTTOV radiative transfer model where microwave surface emissivity over oceans is computed by the FASTEM model. The ocean emissivity is influenced by the emissivity of the salted-water, the wave properties and also the whitecap coverage. It has been shown that, at large wind speeds, RTTOV exhibits an important bias for radiances from microwave imagers that could be linked to a misrepresentation of the satellite pixel fraction covered by foam.
The current FASTEM whitecap fraction depends only upon the 10m wind speed. Several studies have shown that it also depends on other parameters, such as the sea state. In the IFS, the atmospheric and wave models are coupled. Therefore, a comprehensive information on the sea state is readily available to RTTOV. This capability has been used to implement a new whitecap fraction parametrisation depending upon observation time and location.
Given the lack of global in situ observations of the whitecap fraction, the new parametrisation is evaluated within an assimilation experiment where the whitecap fraction estimate is used by RTTOV. Positive results are noticed regarding the first-guess departure biases but the standard deviations are slightly degraded. In order to understand these results, a retrieval of whitecap fraction has been set-up to act as a reference. The analysis of the results unveils deficiencies in other components of the FASTEM model and most likely in the foam emissivity parametrisation.

Acknowledgement This study has been carried out within the context of the EUMETSAT Satellite Application Facility on Numerical Weather Prediction (NWP SAF). The full report of the Visiting Scientist mission (NWP_VS12_02) is availlable on the NWP SAF website (`http://www.nwpsaf.eu/`).

1 Introduction

In current data assimilation systems, satellite observations give the most important contribution to the atmospheric analysis especially over data sparse area such as oceans. For each observation, a model equivalent has to be calculated. Regarding satellite data, brightness temperatures have to be computed from the data assimilation system *a priori* information using a radiative transfer model.

At ECMWF, in the IFS numerical weather prediction system, an incremental 4D-Var formulation is used (see [Courtier et al., 1994] and [Rabier et al., 2000]). The *a priori* information comes from a short range forecast started from the previous analysis. In order to assimilate satellite brightness temperatures, the observation equivalent is calculated using the RTTOV radiative transfer code

(see [Saunders et al., 1999]). At a given frequency in the microwave region, depending on the polarization and viewing angle, the simulated brightness temperature can be expressed as follows:

$$T_B = \tau r T_{\downarrow} + \tau e T_s + T_{\uparrow}, \tag{1}$$

where T_B is the simulated brightness temperature, τ is the atmospheric transmission from the surface to space, e is the surface emissivity, r is the surface reflectivity (often assumed to be equal to $1 - e$), $T_{\downarrow}$ is the atmospheric downward radiation (expressed as a brightness temperature), T_s is the surface skin temperature and $T_{\uparrow}$ is the atmospheric upward radiation (expressed as a brightness temperature). τ, $T_{\downarrow}$, $T_{\uparrow}$ are computed from the model temperature and humidity profiles. T_s is taken from the background state and, over sea, e and r are calculated by the FASTEM emissivity model (see [English and Hewison, 1998] and [Liu et al., 2011]).

Microwave imagers such as SSMI/S aboard DMSP satellites give a valuable information about temperature and moisture near the surface. At these frequencies the atmospheric absorption takes place near the surface in a relatively thin layer of the atmosphere, hence the atmospheric transmission to space τ is high. From Eq. (1) one can see that because of the high value of τ, a significant fraction of the brightness temperature measured by the satellite originates from the surface. Consequently, in order to obtain a useful information from these channels, it is crucial to have an accurate modeling of the surface characteristics (e, r, and T_s).

Over sea, the FASTEM model (currently version 5) is used to estimate the surface emissivity. It takes into account the emissivity of salted water but also the emissivity of the foam that may cover a significant portion of the satellite footprint:

$$e = (1 - W) e_{water} + W e_{foam}, \tag{2}$$

where W is the foam coverage, e_{foam} is the foam emissivity and e_{water} is the foam-free sea water emissivity.

- e_{water} is calculated from the Fresnel equation for a flat specular water surface (surface temperature and salinity being accounted for in the permittivity calculation). Then a two-scale correction is applied to take into account the effect of the surface roughness. The small scale correction, aims to parametrise the effect of small-scale ocean waves that are responsible for Bragg scattering of the signal. The large scale correction is designed to account for reflections due to large scale waves (as computed by a geometric optics model integrated over all wave slope facets). Apart from a viewing angle, polarization and frequency dependence, the two-scale correction is driven by the 10 meters wind speed[1]. The reader may refer to [Liu et al., 2011] for more details.

- e_{foam} comes from an empirical parametrisation based on field measurements.

- W is parametrized using the 10 meter wind speed (see [Monahan and O'Muircheartaigh, 1986]).

At frequencies used by microwave imagers, the foam-free water emissivity is relatively low (especially for the horizontally polarized channels) while the foam emissivity is close to one (on both vertically and horizontally polarized channels). Consequently, even with a small amount of foam the contribution on the total emissivity and to the simulated brightness temperature is large.

An attempt to improve the whitecap fraction parametrisation have been made in FASTEM-4 (see [Liu et al., 2011]). Nonetheless, FASTEM-5 reverted back to the previous formulation (cited

[1]The large scale correction is not only depending on the wind speed but also on the stage of development of the large scale waves, e.g. on the wave age. This is ignored in FASTEM.

above). [Bormann et al., 2012] show that with any of these parametrisations a significant bias remains in high wind speed areas, especially for microwave imagers. Therefore, whitecap fraction parametrisation needs to be further addressed in order to improve the skills of microwave ocean surface emissivity models at high wind speed.

In this document, we examine the impact of a new foam coverage parametrisation on simulated brightness temperatures and evaluate its effect on the accuracy of the atmospheric analyses. In the first part we focus on the foam coverage parametrisation itself and highlight the differences between the current FASTEM-5 parametrisation and the proposed formulation. In the second part, we discuss the impact of the new parametrisation on simulated brightness temperatures. The last part shows some promising results of a first attempt to retrieve the whitecap fraction from satellite measurements.

2 Whitecap fraction parametrisation

2.1 Whitecap fraction calculation from wave model fields

[Anguelova and Webster, 2006] made an extensive survey of wind speed driven foam fraction parametrisations. All are obtained by fitting a wind speed function to an observational dataset. These various parametrisations exhibit a very large spread in modelled whitecap coverage (variations of several orders of magnitude for a given wind speed). Several hypotheses are given to explain such large discrepancies :

- Whitecap fraction parametrisations based on wind speed alone do not account for many factors affecting the whitecap coverage: sea state (swell, significant wave height, wave age, ...), surface currents, atmospheric stability near the surface, salinity, sea surface temperature, surface surfactant concentration...

- Observational datasets used to establish the wind speed based parametrisations can be obtained in very different conditions (warm or cold seas, open ocean or fetch limited areas, ...). This can partly explains the large differences between the various formulations. Moreover these datasets do not cover the whole globe: most of them were obtained in coastal areas and few observations are available in the southern hemisphere;

- The whitecap fraction measurement itself (usually based on photographic analysis) can also lead to uncertainties.

Other parametrisations have been developed in order to better take into account the sea state (see [Goddijn-Murphy et al., 2011] for a review of these parametrisations). In this study we examine a new parametrisation based on wave model outputs. Such models give a detailed description of the full wave spectrum which in turns can be used to provide information on the sea state. Wave models such as the WAM model coupled to IFS (see [Janssen et al., 2005]) are based on the following equation:

$$\frac{DF(\omega,\theta)}{Dt} = S_{in}(\omega,\theta) + S_{nl}(\omega,\theta) + S_{ds}(\omega,\theta), \tag{3}$$

where F is the wave variance spectrum (that depends on the frequency, ω, and direction, θ), S_{in} is the source term for wind input, S_{nl} is for the nonlinear interactions and S_{ds} is the energy dissipation. Bottom friction set aside, it is assumed that wave breaking is the dominant mechanism for energy

dissipation and that each breaking event produces whitecaps. The energy flux from waves to ocean is given by:

$$\Phi_{oc} = \rho_w g \int S_{ds} d\theta d\omega. \tag{4}$$

Following [Kraan et al., 1996], it is possible to calculate the whitecap fraction from the modelled energy flux from waves to ocean:

$$\Phi_{oc} = -\gamma \rho_w g W \omega_p E, \tag{5}$$

where, E is the total wave variance, ω_p is the angular peak frequency, W is the whitecap fraction, γ is the average fraction of the total wave energy dissipated per whitecapping event. Melville and Rapp (1985) suggested a value of $\gamma = 0.005$. This constant value has been chosen in our first attempt to calculate the whitecap fraction.

From eq. (4) and (5), W can be written as:

$$W = -\frac{\Phi_{oc}}{\gamma \rho_w g E \omega_p}, \tag{6}$$

where Φ_{oc}, E and ω_p are calculated by the wave model.

It should be noted that:

- Since the peak angular frequency may jump from one mode to another when wind sea and swells are combined, in practice, ω_p is assumed to be equal to the mean angular frequency of the wind-sea.
- E is linked to the significant wave height H_S by $E = {H_S}^2/16$.

W can also be expressed as a combination of normalized variables:

$$W = -\frac{\epsilon m \chi}{\gamma E_*}, \tag{7}$$

where $\epsilon = \rho_a/\rho_w$, E_* is the dimensionless wave variance $E_* = g^2 E/u_*^4$ (u_* being the friction velocity), m is the normalised dissipation $m = -\Phi_{oc}/\left(\rho_a u_*^3\right)$ and χ is the wave age $\chi = g/(\omega_p u_*)$.

In this whitecap fraction parametrisation, the dependence on the sea state is driven by Φ_{oc}, E and ω_p. There is no direct dependence on the wind speed, but the modeled Φ_{oc} is influenced by it. Restriction to the case of pure wind sea, one can demonstrate that this parametrisation is consistent with the one introduced in [Kraan et al., 1996] where W is roughly proportional to χ^{-2}. Small values of χ indicate young wind-seas whereas large values of χ indicate well developed seas. Consequently, the parametrisation of W defined in Eq. (6) gives higher whitecap fractions for young wind-seas.

This parametrisation based on wave energy dissipation should be able to better represent the whitecap fraction variability compared to the FASTEM-5 parametrisation that is solely based on the 10m wind speed. Nonetheless, parameters like atmospheric stability, salinity, sea surface temperature or surface currents are not taken into account which can lead to noticeable differences between diagnosed and observed whitecap fraction. Even though a few parameters are neglected, because it is linked to the amount of dissipated energy, the new parametrisation should have good skill at predicting the amount of newly generated whitecap (often referred as Stage A foam). On the other hand, the amount of decaying foam (Stage B foam) will be less accurately predicted since the foam decay time greatly vary with parameters such as the surface surfactant concentration or the sea surface temperature (see [Callaghan et al., 2012]).

2.2 Whitecap fraction calculation from IFS/WAM fields

All the necessary input fields are readily available from the ECMWF operational archive. Using short terms forecasts, we have calculated whitecap fraction fields every 6 hours over a 2 months and a half period from 1st October 2012 to 14th December 2012. Mean whitecap fraction fields are presented in Figure 1 using the mean frequency of the wind-sea (a).

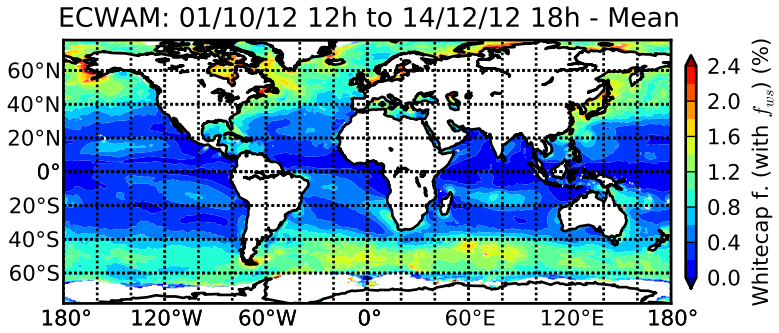

(a) Using the mean frequency of the wind sea

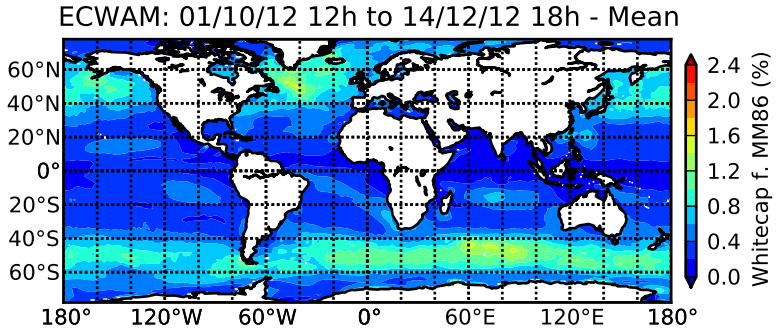

(b) Using the 10m wind speed ([Monahan and O'Muircheartaigh, 1986])

Figure 1: Mean whitecap fraction cubic root field between 1st October 2012 and 14th December 2012, based on short term forecasts of IFS/WAM, computed from various formulations.

Overall, the geographical distribution of the whitecap fraction diagnosed using the WAM model (Fig. 1.a) is close to the one given by the formula based on the wind speed (Fig. 1.b). Near the coasts (Alaska), in sheltered area (Caribbean sea, North Sea, Mediterranean sea, Japan Sea) and in some regions where the ocean is relatively shallow (South of Argentina, North of the China sea), whitecap amounts diagnosed using the WAM model are higher. In those regions, because of the small fetch distance and of finite depth, the wave model produces steeper waves which in turns dissipate more energy.

The wave model based parametrisation, shows a saturation of the whitecap fraction at high wind speeds (see Figure 2). This is in good agreement with the findings of [Goddijn-Murphy et al., 2011] who noticed evidences of such a saturation in field experiment measurements.

2.3 Conclusion

Because of the lack of global measurements of the whitecap fraction, it is difficult at this point to determine which whitecap parametrisation and wave model performs best. The effect of the new whitecap fraction parametrisation on the simulated brightness temperatures can be seen as an indirect validation.

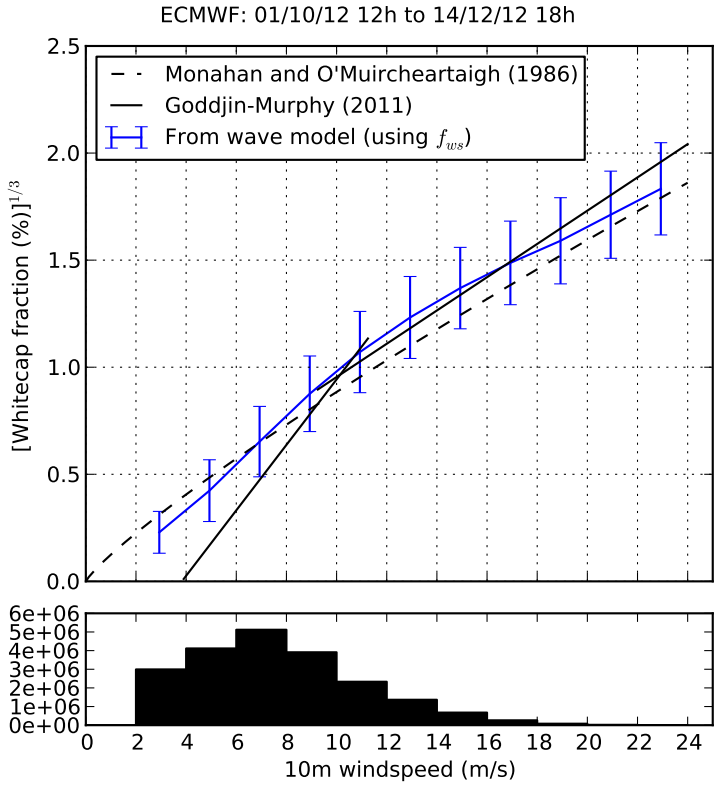

Figure 2: Mean whitecap fraction cubic root, with respect to wind speed, between 1st October 2012 and 14th December 2012. Based on short term forecasts of IFS/WAM. Error bars show the standard deviation.

The IFS code has been modified to allow the online calculation of the whitecap fraction from the wave model fields. Since the atmospheric model and wave model are fully coupled in the IFS, the diagnosed whitecap fraction is available at each model time-step. It can consequently be used by FASTEM during the surface emissivity calculation in an assimilation experiment.

3 Impact on the simulated brightness temperatures in IFS

3.1 Experiments setup

A version of IFS based on cycle 38r2 e-suite has been used. It also includes improved scattering coefficients for the microwave radiative transfer (see [Geer, 2013]). Compared to operations, the atmospheric model has been run at a lower truncation (T511L91) and in the incremental 4D-var algorithm three outer loops have been performed at respectively T95, T159 and T255.

All the observations currently assimilated at ECMWF are used. Regarding satellite data, infrared and microwave sounders are assimilated in clear sky conditions only, whereas microwave imagers are also used in thick and precipitating clouds (see [Bauer et al., 2010] and [Geer et al., 2010]). For satellite and aircraft data, the variational bias correction (VarBC) is used (see [Dee, 2005]). We use the same predictors as in the operational IFS, but we have turned on the passive monitoring on all TRMM/TMI, Coriolis/Windsat and DMSP-F18/SSMIS channels.

Over the period of 1 October 2012 00UTC to the 14 December 2012 12UTC, two experiments have been run:

- `fwas` (also referred as control): a baseline using the current wind-based whitecap fraction parametrisation of FASTEM-5.

- `fw76` (also referred as new): a experiment using the whitecap fraction parametrisation introduced in the previous section, based on the mean frequency of wind sea.

Because of the addition of new monitored channels and of the change for the emissivity calculation in the new experiment, the VarBC coefficients needs a few assimilation cycles to adjust. Based on an examination of the VarBC coefficients time-series (not shown) we discarded the first nine days. The comparison between the two experiments will therefore start from the 10 October 2012 00UTC.

3.2 Overall results

When dealing with data going through the Allsky route, one can define three cloudiness categories summarized in Table 1. For non-cloudy observations, the measured brightness temperature is very sensitive to the surface emissivity. For rainy observations, the atmosphere is nearly opaque. Ideally, in order to evaluate the whitecap fraction impact, one would like to use only non-cloudy observation. However, this sample exhibit a bias toward low wind speed values where the whitecap amount is known to be small. Because of this trade-off between surface sensitivity and 10 m wind speed sampling, we have chosen to focus on all the non-rainy observations.

	LWP threshold	SI threshold	Approx. % of the total
Non-cloudy	$< 0.5 kg/m^2$	$< 40K$	40%
Non-rainy		$< 40K$	90%
Active			100%

Table 1: Cloudiness categories for Allsky observations. (LWP stands for the Liquid Water Path calculated from the 22Ghz V and 37Ghz V channels. SI stands for the scattering index defined as the brightness temperature difference between the 37Ghz V and 37Ghz H channels.)

Results for the TMI imager are shown in Figure 3. At all wind speeds, the mean bias corrected first-guess departure is nearly unchanged. However, for low frequencies at high wind speeds the first-guess departures standard deviation are degraded when the new whitecap fraction parametrisation is used. This is not the case for the high frequency channels (around 90GHz) that are less sensitive to the surface.

Results for the SSMI/S imaging channels aboard DMSP F17 and F18 are shown in Figure 4. SSMI/S has a global coverage whereas TMI only covers the area between 40°S and 40°N. SSMI/S extended coverage allows to sample more high wind speed scenes so that the statistics for the 20-25m/s wind speed bin are shown in the plots of Figure 4. Statistics for SSMI/S and TMI are quite similar. The statistics for the highest wind speeds confirms that the new whitecap fraction parametrisation gives slightly degraded results especially for the low frequency channels that are also the more sensitive to the surface emission.

For both TMI and SSMI/S, the plots show that overall, at low frequencies, the bias correction becomes less dependent on the 10m wind speed. This is backed up by the fact that VarBC coefficients for the 10m wind speed predictor are smaller in the experiment using the new whitecap fraction parametrisation.

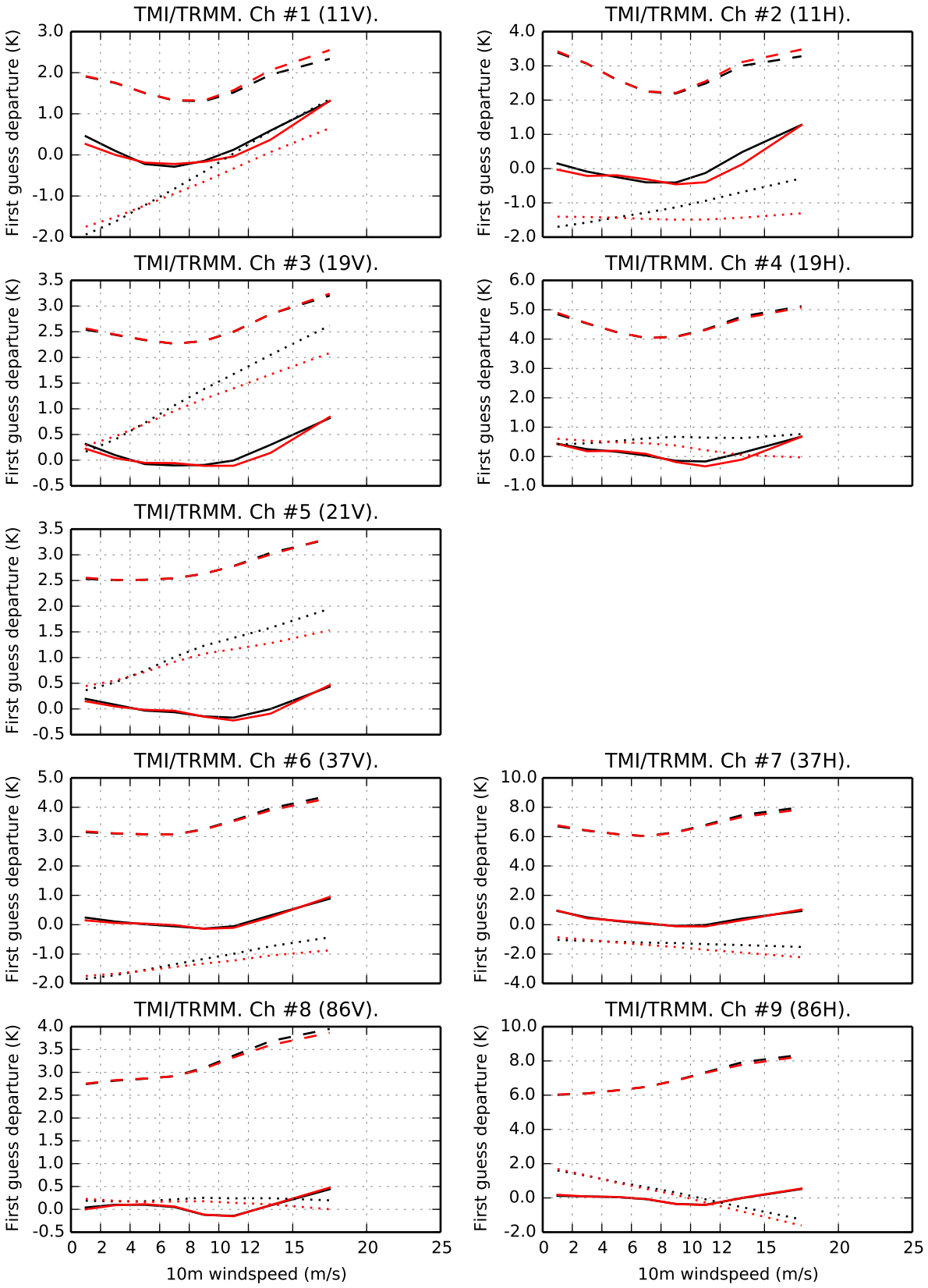

Figure 3: First guess departure as function of the 10m wind speed for the TRMM/TMI imager between the 10 October 2012 and the 14 December 2012 for all the non-rainy radiances. The reference run is plotted in black, the new experiment is plotted in red. Mean departures, bias correction and departures standard deviation are respectively plotted in plain, dotted and dashed lines.

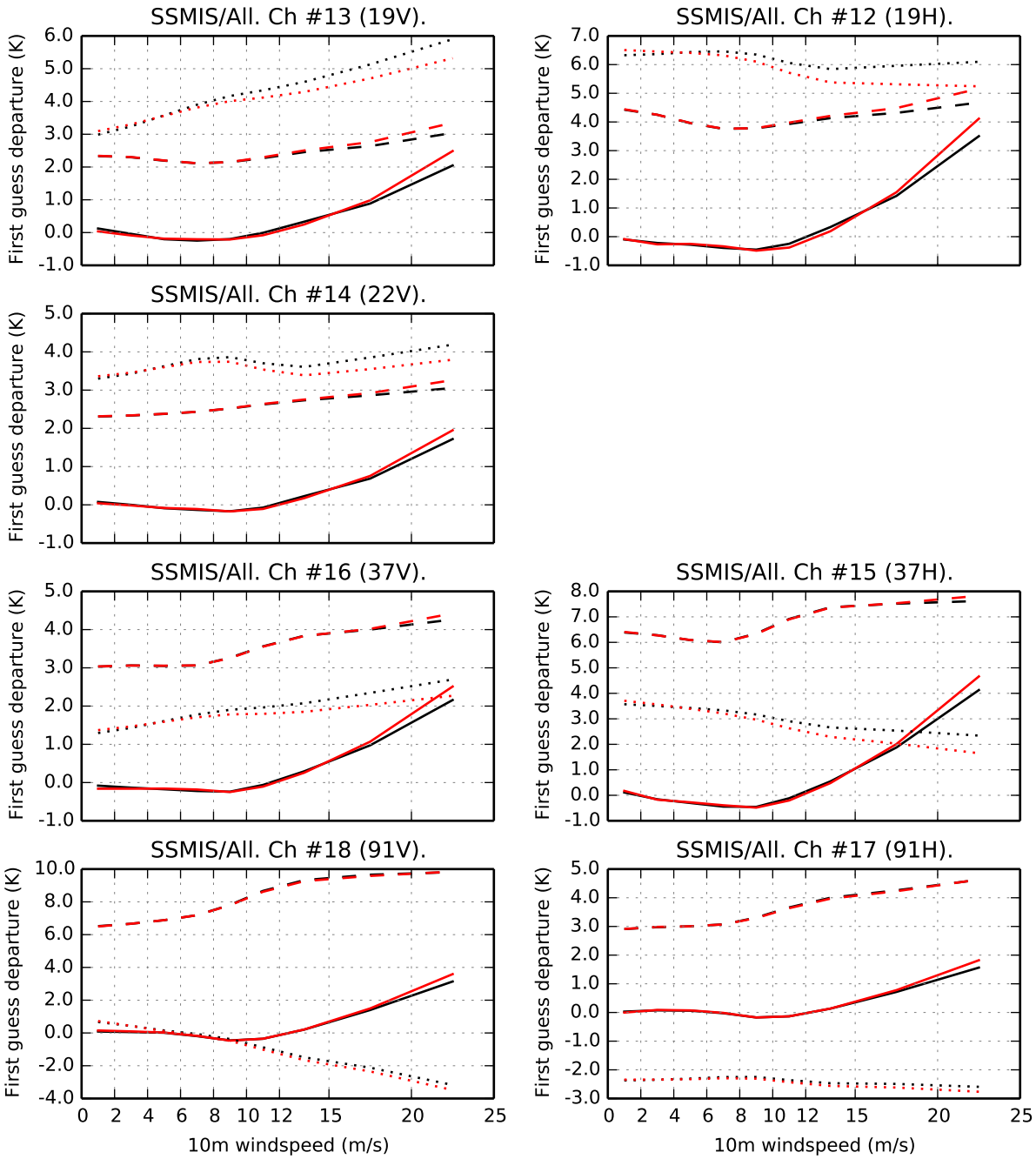

Figure 4: First guess departure as function of the 10m wind speed for the SSMI/S imager aboard DMSP-F17 and F18 between the 10 October 2012 and the 14 December 2012 for all the non-rainy radiances. The reference run is plotted in black, the new experiment is plotted in red. Mean departures, bias correction and departures standard deviation are respectively plotted in plain, dotted and dashed lines.

3.3 Geographical distribution

Statistics for TMI and SSMI/S have been aggregated on a 2.5°x2.5° lat/lon grid during the trial period (from 10 October 2012 to 14 December 2012). For the SSMI/S imaging channels (vertical polarisation only), Figure 5 shows the difference of the absolute values of the bias corrected first-guess departure between the new and the reference experiment. At frequencies between 19 and 37 GHz, for both polarisations, the mean first guess departure is increasing in several coastal areas and/or sheltered seas (Caribbean Sea, Tip of Argentina, China sea, Mediterranean sea).

Over the North Atlantic ocean and the South Indian ocean, the standard deviation of the first-guess departures tends to increase when the new whitecap fraction parametrisation is used (maps not shown). This is in good agreement with Figure 4 since high wind speed values are usually observed in those regions

Statistics from TMI (maps not shown) lead to similar conclusions.

3.4 Summary

The use of a whitecap fraction diagnosed from the wave model outputs, gives us promising results regarding the bias of the radiative transfer simulations with respect to the wind speed. However, the whitecap fraction parametrisation still needs to be improved. The degradation of the first-guess departures standard deviation at high wind speed, might be reduced by a better tuning of the parametrisation.

The increase of the first-guess departures biases in coastal and sheltered areas is probably linked to an excess of whitecap. In section 2.2, this has been explained by the fact that, in such areas, waves are steeper which leads to a higher amount of dissipated energy. Since, the γ parameter in Eq. 5 has been set to a constant value in our experiment, this translates directly into higher amounts of whitecap. Therefore, a way to tune the whitecap fraction parametrisation would be to consider γ as a function of the wave steepness or more generally of the sea state.

4 Whitecap fraction retrieval

4.1 Retrieval method and experiment setup

Whitecap fraction retrievals from microwave imager measurements have already been successfully used to derive statistics on the global whitecap coverage (see [Anguelova and Webster, 2006]). In FASTEM-5, the emissivity is calculated as follows:

$$e = (1 - W)e_{water} + We_{foam}, \tag{8}$$

where, e_{water} and e_{foam} are either calculated or empirically parametrised in FASTEM. [Prigent et al., 2005] and [Karbou et al., 2006] have demonstrated that it was possible to retrieve the total emissivity from satellite measurements. Therefore, given our knowledge of e_{water} and e_{foam} it is possible to retrieve the whitecap fraction W.

The IFS experiment used for the whitecap retrieval (`fwl6`) is configured in a similar manner to the new experiment (`fw76`) described in section 3.1. However, in the VarBC setup, the use of the 10 m wind speed predictor has been removed. Using the 10 m wind speed predictor would lead to unrealistic whitecap fraction estimates since the observed brightness temperature used during the emissivity retrieval would be bias corrected for the whitecap fraction parametrisation deficiencies.

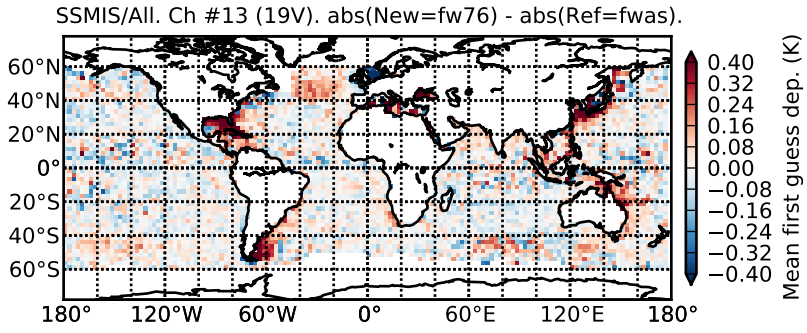

(a)

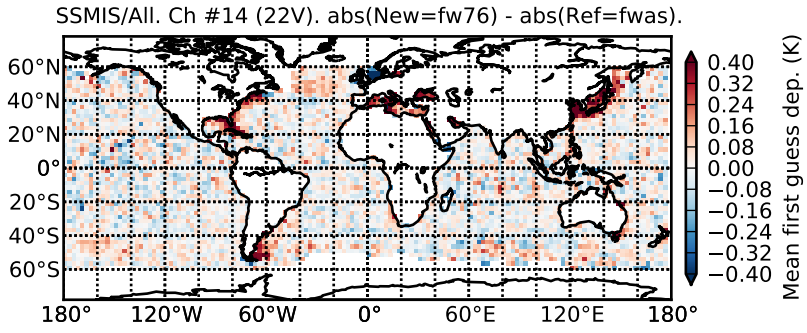

(b)

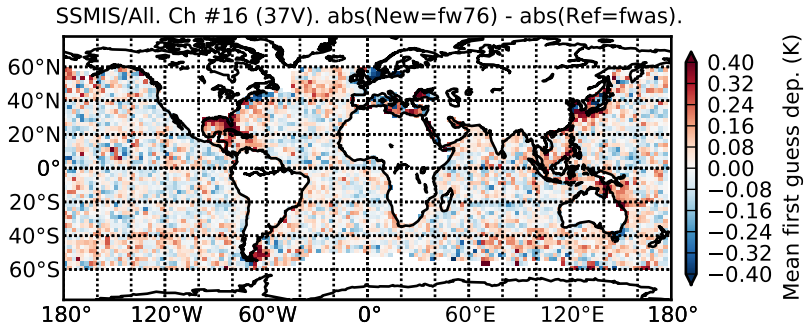

(c)

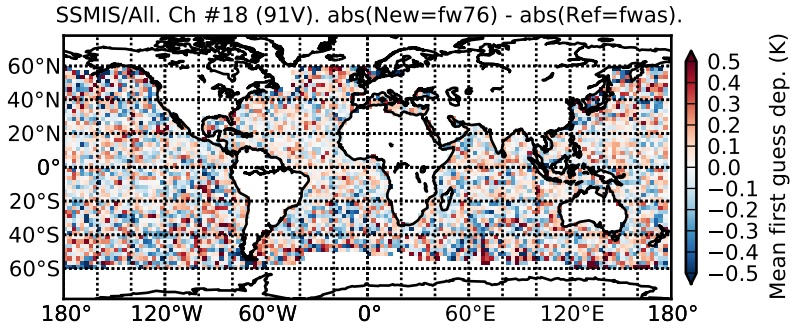

(d)

Figure 5: Mean first-guess departures absolute difference for the SSMI/S imager aboard DMSP-F17 and F18 between the new and the reference experiment. Only the vertically polarised channels are shown here.

The accuracy of the emissivity retrieval strongly depends on the accuracy of the IFS first guess and of the RTTOV simulation. To avoid cases where the atmosphere is nearly opaque, we will consider only the non-rainy radiances (see Table 1) with a more stringent threshold on the scattering index (50 K instead of 40 K).

4.2 Validity of the results

For each sensor and frequency, the retrieved whitecap fraction can be averaged on a 2.5°x2.5° lat/lon grid for the experiment duration (between the 10 October 2012 and the 14 October 2012). Independently, we apply the same sampling to the whitecap fraction diagnosed from the wave model.

At low frequencies (10 to 22 GHz), the geographical distribution of the mean retrieved whitecap fraction is in good agreement with the diagnosed whitecap fraction (see Figure 6). In this range of frequency, results are consistent across sensor types (TMI, SSMI/S and WindSat) and polarisations. In section 3.3, when the new whitecap fraction parametrisation is used, we have noticed a degradation of the first-guess departures in some coastal and sheltered areas. That was linked to an increase in the whitecap amount compared to the wind-based formula. The whitecap fraction retrieval shows no evidence of such an increase in the whitecap amount which confirm the need of re-tuning of the new whitecap fraction parametrisation.

At higher frequencies (37 and 90GHz), the whitecap retrievals are dominated by biases in the radiative transfer and model (not shown). At 37GHz, marine stratocumulus in the trade wind areas seem to be the main cause of bias. At 90GHz, excessive amount of whitecap are also diagnosed under the thicker clouds around the ITCZ and PTCZ. Consequently, we will not use whitecap retrievals at such high frequencies.

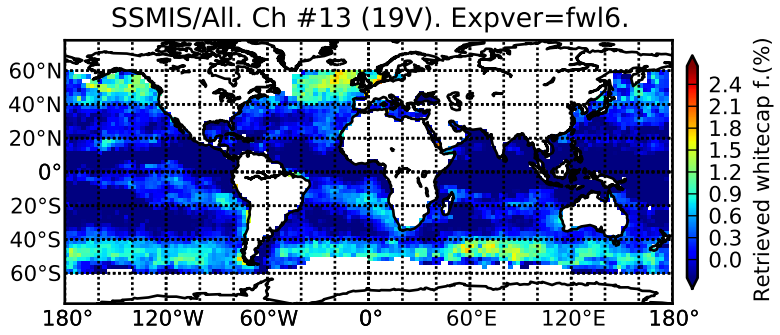

(a) Retrieved whitecap fraction

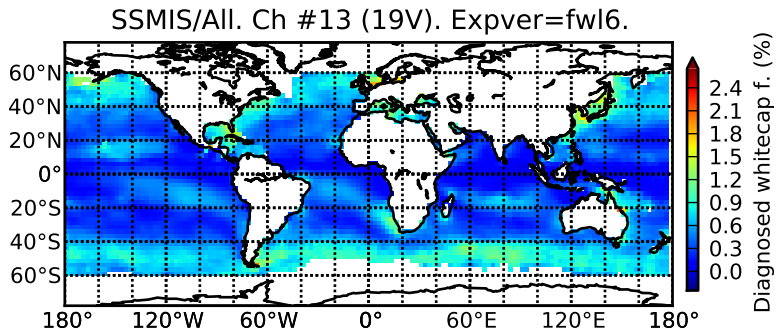

(b) Diagnosed whitecap fraction (from the wave model)

Figure 6: Mean retrieved and diagnosed whitecap fraction for SSMI/S channel 2 (19 GHz V) aboard DMSP F17 and F18

Statistics with respect to the 10 m wind speed (see Figure 7) show that uncorrected biases remain in the atmospheric model or radiative transfer code. Indeed, especially at low wind speeds, negative mean whitecap fractions are obtained: since in the retrieval experiment there is no VarBC predictor based on the 10 m wind speed, VarBC ensures that the bias is corrected when all wind speeds are considered but this does not guarantee that the bias is null for a given wind speed (notably at 0 m/s). This causes the offset on the whitecap fraction retrieval curves but does not affect the shape of the curves.

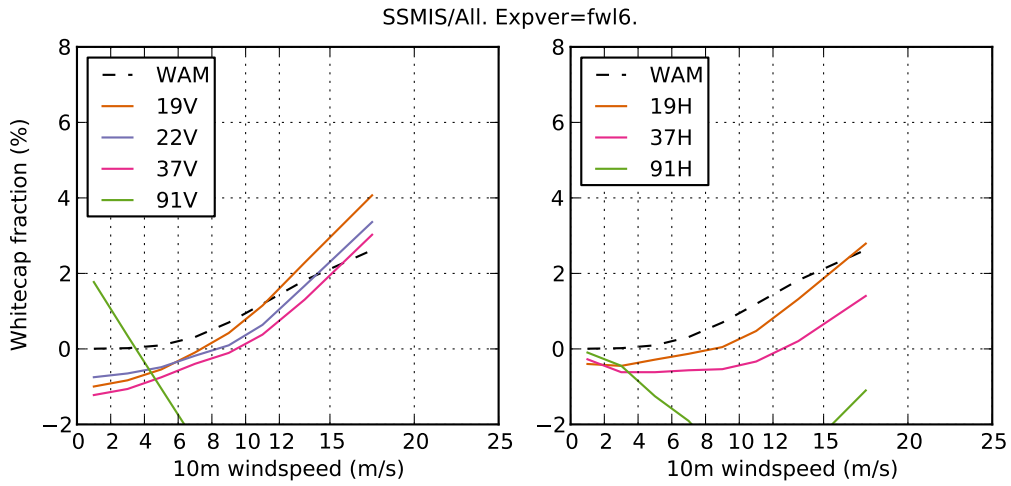

(a) SSMI/S aboard DMSP F17 and F18

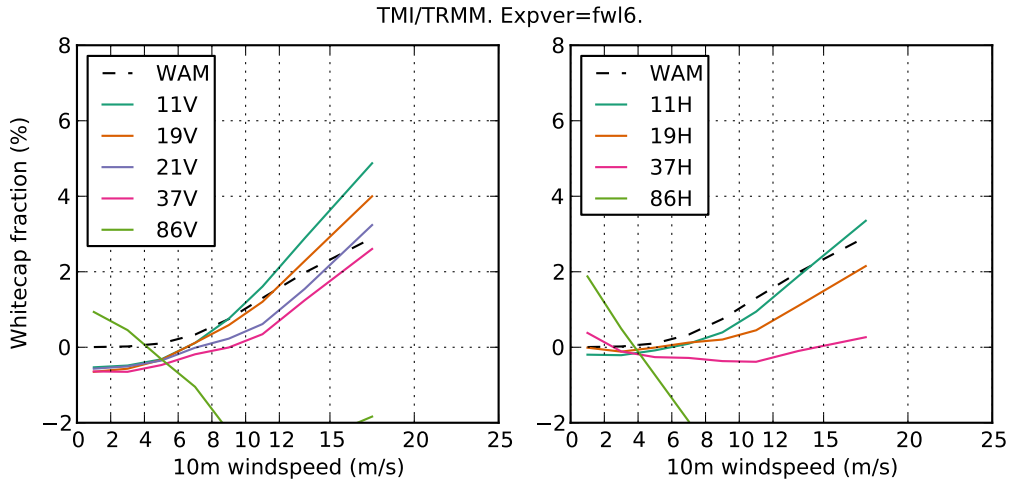

(b) TMI aboard TRMM

Figure 7: Retrieved whitecap fraction for the SSMI/S and TMI sensors with respect to the wind speed.

Figure 7 shows that the retrieved whitecap fraction varies with frequency and polarisation. At a given frequency and for high incidence angle (around 53° for SSMI/S and TMI), the emissivity of the foam is significantly smaller for the horizontal polarisation than for the vertical one. Such a difference between the two polarisations is taken into account in the FASTEM foam emissivity parametrisation, however the comparison to laboratory measurements (see [Rose et al., 2002]) suggests that the emissivity for the horizontal polarisation might be overestimated in FASTEM which would explain the lower amount of retrieved whitecap for the horizontal polarisations.

For a given polarisation, the retrieved whitecap fraction decreases with increasing frequencies. This could arise from an improper parametrisation of the foam emissivity in FASTEM where the emissivity increases with the frequency. Indeed, [Rose et al., 2002] laboratory measurements at 10.8 and 36.5GHz show no evidence of such an increase.

In this study, we have exclusively studied mean values of the retrieved whitecap fraction (for specific wind speeds and locations). In theory, the retrieved whitecap fraction could give us an indication about the statistical distribution of the whitecap fraction for a given wind speed. This would help to evaluate the ability of the wave model based parameterisation to take into account the sea state (that is currently ignored in FASTEM). However, prior to such an evaluation, the error of the whitecap fraction retrieval itself should be carefully examined. Indeed, the spread of the retrieved whitecap fraction is greatly influenced by the quality of the background fields used for the retrieval or by the quality of the other components of the radiative transfer model.

4.3 Summary

Emissivity retrievals are a valuable tool to evaluate the biases of whitecap parametrisations over a given area. Moreover, the comparison between retrieved whitecap amounts at various frequencies and polarisations gives an insight on the performances of the emissivity models for the foam and the foam-free water.

Retrievals at low frequencies confirm results of section 3.3 in coastal and sheltered areas. Moreover, overall statistics stress out the need of additional work on the emissivity model of the foam. The current parametrisation of the foam emissivity is based on Stogryn empirical model and has been modified in FASTEM-4. However, compared to laboratory measurements, differences remain and need to be addressed. This work on the foam emissivity would benefit to all whitecap parametrisations.

5 Conclusion and perspectives

In the present study, a whitecap fraction parametrisation based on wave model outputs have been applied to the ECMWF wave model (WAM). This new parametrisation gives realistic results. However the lack of *in situ* observations makes a direct evaluation of this parametrisation very difficult.

As an indirect validation, we have implemented this new whitecap fraction parametrisation in a development branch of the IFS model which allows us to run assimilation experiments using the new whitecap fraction estimate in the RTTOV radiative transfer code. In terms of total bias, results are improved. However the standard deviation of the first guess departures are slightly degraded at high wind speeds for surface sensitive channels. Moreover, the new parametrisation seems to generate excessive whitecap amounts in several coastal and sheltered areas.

In order to understand the new whitecap fraction parametrisation weaknesses and because of the lack of *in situ* observations, a whitecap fraction retrieval was attempted. It gives promising results for low frequency imaging channels and allows us to confirm the new parametrisation deficiencies in coastal and sheltered areas. Unexpectedly, it also pointed out the need of a revised foam emissivity parametrisation within FASTEM.

Recent laboratory measurements of the foam emissivity may be used to update the current empirical foam emissivity parametrisation. However, in the literature, measurements are usually available only at low frequencies. A more innovative approach would be to use physically-based foam emissivity models such as the one developed at NRL (see [Anguelova, 2008] and [Anguelova et al., 2009]).

Physically-based models might be computationally too expensive to be integrated in FASTEM but could be used to derived a new regression-based parametrisation.

References

[Anguelova et al., 2009] Anguelova, M., Gaiser, P., and Raizer, V. (2009). Foam emissivity models for microwave observations of oceans from space. In *Geoscience and Remote Sensing Symposium,2009 IEEE International,IGARSS 2009*, volume 2, pages II–274–II–277.

[Anguelova, 2008] Anguelova, M. D. (2008). Complex dielectric constant of sea foam at microwave frequencies. *Journal of Geophysical Research: Oceans*, 113(C8):n/a–n/a.

[Anguelova and Webster, 2006] Anguelova, M. D. and Webster, F. (2006). Whitecap coverage from satellite measurements: A first step toward modeling the variability of oceanic whitecaps. *Journal of Geophysical Research: Oceans*, 111(C3).

[Bauer et al., 2010] Bauer, P., Geer, A. J., Lopez, P., and Salmond, D. (2010). Direct 4d-var assimilation of all-sky radiances. part i: Implementation. *Quarterly Journal of the Royal Meteorological Society*, 136(652):1868–1885.

[Bormann et al., 2012] Bormann, N., Geer, A., and English, S. (2012). Evaluation of the microwamicrowave ocean surface emissivity model FASTEM-5 in the IFS. Technical Report Memorandum 667, Research Department, ECMWF, Reading, U. K.

[Callaghan et al., 2012] Callaghan, A. H., Deane, G. B., Stokes, M. D., and Ward, B. (2012). Observed variation in the decay time of oceanic whitecap foam. *Journal of Geophysical Research: Oceans*, 117(C9).

[Courtier et al., 1994] Courtier, P., Thépaut, J.-N., and Hollingsworth, A. (1994). A strategy for operational implementation of 4d-var, using an incremental approach. *Quarterly Journal of the Royal Meteorological Society*, 120(519):1367–1387.

[Dee, 2005] Dee, D. P. (2005). Bias and data assimilation. *Quart. J. Roy. Meteor. Soc.*, 131(613):3323–3343.

[English and Hewison, 1998] English, S. J. and Hewison, T. J. (1998). Fast generic millimeter-wave emissivity model. *Proc. SPIE, Microwave Remote Sensing of the Atmosphere and Environment*, 3508:288–300.

[Geer, 2013] Geer, A. J. (2013). All-sky assimilation: better snow-scattering radiative transfer and addition of ssmis humidity sounding channels. Technical Report 706, ECMWF.

[Geer et al., 2010] Geer, A. J., Bauer, P., and Lopez, P. (2010). Direct 4d-var assimilation of all-sky radiances. part ii: Assessment. *Quarterly Journal of the Royal Meteorological Society*, 136(652):1886–1905.

[Goddijn-Murphy et al., 2011] Goddijn-Murphy, L., Woolf, D. K., and Callaghan, A. H. (2011). Parameterizations and algorithms for oceanic whitecap coverage. *J. Phys. Oceanogr.*, 41(4):742–756.

[Janssen et al., 2005] Janssen, P., Bidlot, J.-R., Abdalla, S., and Hersbach, H. (2005). Progress in ocean wave forecasting at ECMWF. Technical Report Memorandum 478, Research Department, ECMWF, Reading, U. K.

[Karbou et al., 2006] Karbou, F., Gérard, E., and Rabier, F. (2006). Microwave land emissivity and skin temperature for amsu-a and -b assimilation over land. *Quarterly Journal of the Royal Meteorological Society*, 132(620):2333–2355.

[Kraan et al., 1996] Kraan, C., Oost, W., and Janssen, P. (1996). Wave energy dissipation by whitecaps. *Journal of Atmospheric and Oceanic Technology*, 13(1):262–271.

[Liu et al., 2011] Liu, Q., Weng, F., and English, S. (2011). An improved fast microwave water emissivity model. *Geoscience and Remote Sensing, IEEE Transactions on*, 49(4):1238–1250.

[Monahan and O'Muircheartaigh, 1986] Monahan, E. C. and O'Muircheartaigh, I. G. (1986). Whitecaps and the passive remote sensing of the ocean surface. *International Journal of Remote Sensing*, 7(5):627–642.

[Prigent et al., 2005] Prigent, C., Chevallier, F., Karbou, F., Bauer, P., and Kelly, G. (2005). Amsu-a land surface emissivity estimation for numerical weather prediction assimilation schemes. *J. Appl. Meteor.*, 44(4):416–426.

[Rabier et al., 2000] Rabier, F., Järvinen, H., Klinker, E., Mahfouf, J.-F., and Simmons, A. (2000). The ecmwf operational implementation of four-dimensional variational assimilation. i: Experimental results with simplified physics. *Quarterly Journal of the Royal Meteorological Society*, 126(564):1143–1170.

[Rose et al., 2002] Rose, L., Asher, W., Reising, S., Gaiser, P., St Germain, K., Dowgiallo, D., Horgan, K., Farquharson, G., and Knapp, E. (2002). Radiometric measurements of the microwave emissivity of foam. *Geoscience and Remote Sensing, IEEE Transactions on*, 40(12):2619–2625.

[Saunders et al., 1999] Saunders, R., Matricardi, M., and Brunel, P. (1999). An improved fast radiative transfer model for assimilation of satellite radiance observations. *Quarterly Journal of the Royal Meteorological Society*, 125(556):1407–1425.